$(dT)_{12-18}$, and poly(rC) · oligo$(dG)_{12-18}$. Ten microliters of virus (which was concentrated 100-fold by centrifugation and then suspended in 50 m*M* tris-HCl, *p*H 7.3, 10 m*M* dithiothreitol, and bovine serum albumin, 1 mg/ml) were incubated with 10 $\mu$l of 50 m*M* tris-HCl, *p*H 7.3, 10 m*M* dithiothreitol, 0.06 percent Triton X-100 for 10 minutes at 2°C. A portion (20 $\mu$l) of assay mixture was added, and the resulting 40-$\mu$l reaction mixture was incubated for 60 minutes at 37°C. The reaction was stopped by the addition of 0.5 ml of 80 m*M* sodium pyrophosphate, 25 $\mu$l of bovine serum albumin (5 mg/ml), and 0.5 ml of 25 percent trichloroacetic acid at 2°C. Acid-insoluble material was collected on glass fiber filters, washed extensively with 10 percent trichloroacetic acid, dried, and dissolved in NCS tissue solubilizer; the radioactivity was then counted in toluene-based scintillation fluid. The reaction mixtures with poly(rA) · oligo$(dT)_{12-18}$ and poly(dA) · oligo$(dT)_{12-18}$ consisted of: 50 m*M* tris-HCl, *p*H 7.3, 70 m*M* KCl, 10 m*M* dithiothreitol, 0.1 m*M* each of deoxyriboadenosine triphosphate (dATP), deoxyriboguanosine triphosphate (dGTP), deoxyribocytidine triphosphate (dCTP), 2.3 $\mu M$ $^3$H-labeled thymidine triphosphate (40,000 count/min per picomole), 20 $\mu$g of poly(rA) or poly(dA) per milliliter, 20 $\mu$g of oligo$(dT)_{12-18}$ per milliliter, and either 5 m*M* $MgCl_2$ or 0.4 m*M* $MnCl_2$. The reaction mixture containing poly(rC) · oligo$(dG)_{12-18}$ consisted of: 50 m*M* tris-HCl, *p*H 7.3, 50 $\mu$g of actinomycin D per milliliter, 15 m*M* KCl, 10 m*M* dithiothreitol, 10.7 $\mu M$ $^3$H-labeled dGTP (6500 count/min per picomole), 40 $\mu$g of poly(rC) per milliliter, 40 $\mu$g of oligo$(dG)_{12-18}$ per milliliter, and either 25 m*M* $MgCl_2$ or 0.4 m*M* $MnCl_2$.


11. R. C. Nowinski, E. Edynak, N. H. Sarkar, *Proc. Natl. Acad. Sci. U.S.A.* **68**, 1608 (1971); H. C. Chopra, I. Zelljadt, E. M. Jensen, M. M. Mason, N. J. Woodside, *J. Natl. Cancer Inst.* **46**, 127 (1971).
12. N. C. Goodman and S. Spiegelman, *Proc. Natl. Acad. Sci. U.S.A.* **68**, 2203 (1971).
13. J. W. Abrell and R. C. Gallo, *J. Virol.* **12**, 431 (1973).
14. J. Schlom and S. Spiegelman, *Science* **174**, 840 (1971).
15. Serum was neutralized by titrating the virus on FCf2Th cells before and after reacting serial tenfold dilutions of virus with an equal volume of antiserum diluted 1 : 5 at room temperature for 1 hour. Inoculated cultures were split 1 : 10 by trypsinization at weekly intervals. After two passages, RDDP activity in the culture fluids was determined. The titer of the virus was $10^{4.5}$ tissue culture infective doses (50 percent effective) per 0.1 ml with and without serum. The antiserum used was prepared in goats against intact virus and was obtained from Dr. R. Wilsnack, Huntingdon Research Center, Brooklandville, Md. Mouse mammary tumor virus, baboon type C virus (M7), and woolly monkey sarcoma virus antiserums from the same source also failed to neutralize the squirrel monkey virus when similarly tested.
16. P. K. Nakane and G. B. Pierce, *J. Histochem. Cytochem.* **14**, 929 (1966); E. H. Leduc, R. Wicker, S. Aurameus, W. Bernhard, *J. Gen. Virol.* **4**, 609 (1969).
17. The rabbit antiserum to M-PMV polymerase was supplied by Dr. M. Ahmed, Pfizer Inc., Maywood, N.J.
18. K. H. Rand and C. Long, *Nature New Biol.* **240**, 187 (1972).
19. M. Ahmed, G. Schidlovsky, D. L. Larson, M. Manousos, S. A. Mayyasi, *J. Gen. Virol.* **30**, 11 (1976).
20. A. F. Bykovsky, I. S. Irlin, V. M. Zhdanov, *Arch. Gesamte Virusforsch.* **45**, 144 (1974).
21. R. S. Howk, L. A. Rye, L. A. Killeen, E. M. Scolnick, W. P. Parks, *Proc. Natl. Acad. Sci. U.S.A.* **70**, 2117 (1973); D. H. Moore, *Cancer Res.* **34**, 2322 (1974); A. S. Dion, A. B. Vaidya, G. S. Fout, *ibid.*, p. 3509; D. L. Fine and L. O. Arthur, *Abstr. Annu. Mtg. Am. Soc. Microbiol.* (1974), p. 246 (V273); R. Michalides, J. Schlom, J. Dahlberg, K. Perk, *J. Virol.* **16**, 1039 (1975).
22. A. Hellman *et al.*, *J. Virol.* **14**, 133 (1974); K. H. Rand, C. W. Long, T. T. Wei, R. V. Gilden, *J. Natl. Cancer Inst.* **53**, 449 (1974).
23. J. Schlom, G. Schochetman, D. Colcher, W. Drohan, Abstracts, VII International Symposium on Comparative Leukemia Research No. C-11 (1975); D. Colcher, W. Drohan, J. Schlom, *J. Virol.* **17**, 705 (1976).


24. Supported by contract NO1-CP-43214 within the Virus Cancer Program, National Cancer Institute. We thank A. Bodenman, C. Thomas, and G. Peacher for technical assistance.

18 June 1976; revised 15 July 1976


# Sodium-Specific Membrane Channels of Frog Skin Are Pores: Current Fluctuations Reveal High Turnover


Abstract. *The reversible sodium transport blocker amiloride causes current fluctuations at the apical membrane of the outer stratum granulosum of frog skin. Their power density spectra reveal that single transport sites translocate more than $10^6$ sodium ions per second, which indicates a pore mechanism. The density of open plus amiloride-blocked pores is in the order of $10^8$ pores per square centimeter of skin area with 60 millimolar sodium and 18 micromolar amiloride in the outer solution.*


Carrier- and pore-mediated transport through biological membranes can be distinguished by the turnover number of individual transport sites (*1*). While a carrier molecule, which has to move through the lipid phase of the membrane, is not likely to transport more than $10^4$ ions or molecules per second, the transport rate of a pore can be several orders of magnitude larger (*2*). Applying this idea to the Na-selective membrane of frog skin, we have attempted to determine the Na turnover of individual transport sites by an evaluation of current fluctuations. The fluctuations were introduced artificially by addition of the drug amiloride, a pyrazine diuretic known to block Na transport reversibly from the outside (*3*). A reversible blocker can be expected to randomly interrupt the Na turnover of individual transport sites. A site will then either conduct fully or, when blocked, not conduct at all. The continuous current *i* passing one site is thus chopped up into small current pulses of varying duration but equal amplitude (*i*). The pulses add up to a mean current which on close inspection will show random fluctuations. The mean current per square centimeter will be

$$I_{Na} = iMP_o \quad (1)$$

where $M$ ($cm^{-2}$) is the mean density of unblocked plus amiloride-blocked transport sites. The steady-state probability $P_o$ represents the fraction of $M$ not blocked by amiloride and $MP_o$ the mean density of open sites. Statistical evaluation of the fluctuations permits computation of *i* and thus the Na turnover of individual transport sites in the open state.

Isolated abdominal skin of *Rana esculenta* was used at room temperature. It was mounted in a Lucite chamber which left 3 $cm^2$ exposed to the bathing solutions. The outer solution was K or Na sulfate Ringer solution containing varying concentrations of amiloride. The inner one was K sulfate Ringer solution, which can be expected to depolarize the K-selective inward-facing membranes of the epithelium and to increase their conductance. Thus, transepithelial resistance and potential were largely determined by the apical membrane of the stratum granulosum (*4*). The current component that did not pass the Na-specific channels was determined as the current flowing in the presence of 35 $\mu M$ amiloride, and was subtracted from the total current to obtain the transcellular Na current, $I_{Na}$.

Transepithelial voltage was clamped to 0 mv by a voltage clamp circuit with continuous feedback. The input stage of the voltage-sensing amplifier was designed around a matched pair of low-noise transistors (National Semiconductor 2N4250) to minimize feedback current fluctuations arising from this stage. The open-loop clamp gain was 25,000. The short-circuit current was amplified with a gain of 50 $\mu$v/na, fed through a high-pass RC-filter with a characteristic frequency of 0.007 hertz, amplified 400 times, and recorded on magnetic tape. Recording periods were 10 to 30 minutes for each amiloride concentration.

The amplified a-c current signal was sampled from the magnetic tape at frequencies of 50 and 5000 hertz by use of an anti-aliasing filter of the Butterworth type (72 db per octave, characteristic frequency set at 80 percent of the maximal analyzed frequency). The digitized signal was divided into 20 records of 4096 words each. A power density spectrum was computed from each record on an IBM 370/58 by use of a fast Fourier transform program. The spectra of 20 records were averaged.

Figure 1A shows five power density spectra in the range 0.3 to 100 hertz. Curves a to d were obtained with a sodium activity of $(Na)_o$ = 60 m*M* in the outer solution and amiloride concentrations of $(A)_o$ = 1.4, 4.3, 12.7, and 35 $\mu M$. Spectrum e was obtained with $(Na)_o$ = 0. Spectra a to d are of the Lorentz type expected for exponential relaxation phenomena. They obey the relationship

$$S = S_o/[1 + (f/f_c)^\alpha] \quad (2)$$

where $S$ is the power density ($amp^2$ sec), $S_o$ the plateau value, $f$ the frequency (hertz), and $f_c$ the corner frequency. The exponent $\alpha$ was found to be in the range 1.75 to 2 (1.8 in Fig. 1A). It is evident

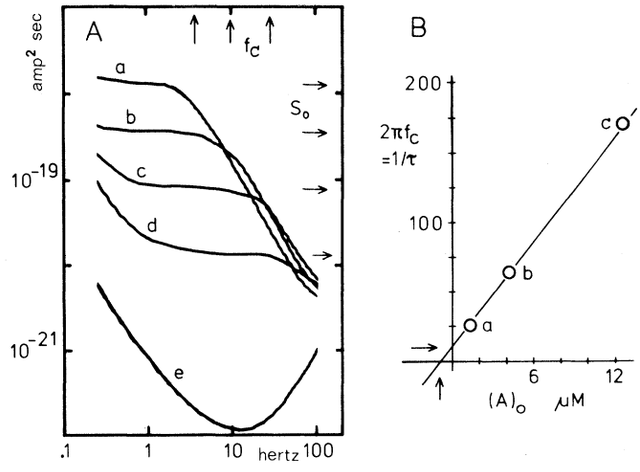


Fig. 1. (A) Power density spectra obtained from 3 cm² of epithelium. Only the parts of the recorded spectra that are relevant for the arguments of this report are shown. (Curves a to d) Increasing amiloride concentrations of $(A)_o$ = 1.4, 4.3, 12.7, and 35 $\mu M$ at 60 m$M$ $(Na)_o$. (Curve e) Sodium-free outer solution (Na replaced by K). The corresponding values of transcellular Na current are (from curve a to curve e) 41, 24, 9, 0, and 0 $\mu$a per 3 cm². The transcellular Na current at $(A)_o$ = 0 was 78 $\mu$a per 3 cm² (spectrum not shown). Plateau values ($S_0$) and corner frequencies ($f_c$) are indicated with horizontal and vertical arrows; $f_c$ was read off where the power density equaled half of the plateau value. The $f_c$ of curve d (for which $I_{Na}$ was zero) was not evaluated because the $\alpha$ value of this curve fell clearly below the expected range. (B) Relationship between corner frequency and amiloride concentration (see Eq. 4a). Arrows point to the intercepts where $k_2$ and $K_A'$ are read off. The linear dependence of $1/\tau$ on $(A)_o$ shows, in retrospect, that neglecting the term $k_1(R)$ in Eq. 4 was justified.

that the plateau value, $S_0$, of the power spectrum decreases with increasing amiloride concentration while the corner frequency $f_c$ increases.

Following a derivation in Verveen and DeFelice (*5*), we may set $2\pi f_c$ equal to the chemical rate $(1/\tau)$ of the current-modulating process. In the simplest possible case this process is due to the random formation and disintegration of a transport-blocking complex between amiloride (A) and the transport site (R)

$$A + R \underset{k_2}{\overset{k_1}{\rightleftarrows}} AR$$

where AR is the blocked site; $k_1$ and $k_2$ are rate constants, and their ratio $K_A = k_2/k_1$ is the dissociation constant of AR. With $M = R + AR$, where $R$ and $AR$ are the densities of unblocked and blocked sites, we find from the law of mass action the steady-state probabilities that a site is unblocked or blocked

$$P_o = R/M = 1/[1 + (A)_m/K_A]$$
$$P_A = AR/M = P_o(A)_m/K_A \quad (3)$$

where $(A)_m$ is the effective amiloride concentration at the outer surface of the membrane. This blocking mechanism implies the following relationship between chemical rate and equilibrium concentrations of A and R (*6*)

$$1/\tau = k_1(A)_m + k_1(R) + k_2 \quad (4)$$

in which (R) is the equilibrium concentration of unblocked transport sites, expressed in the same units as $(A)_m$. In cases where (R), which decreases with increasing $(A)_m$, is numerically negligible compared to $(A)_m$, a linear relationship between amiloride concentration and chemical rate will be expected. We thus obtain the prediction

$$2\pi f_c = 1/\tau = k_1(A)_m + k_2 = k_1\beta(A)_o + k_2 \quad (4a)$$

where $\beta = (A)_m/(A)_o$ is the unknown partition coefficient of amiloride between the outer bulk solution and the space at the outer surface of the membrane. After substituting $\beta$ into Eq. 3 and combining Eq. 3 with Eq. 4a, we find the "on" and "off" probabilities to be

$$P_o = 1/[1 + (A)_o/K_A'] = k_2\tau$$
$$P_A = P_o(A)_o/K_A' = k_1'\tau(A)_o \quad (3a)$$

The linear relationship between $f_c$ and $(A)_o$ predicted by Eq. 4a was found in most experiments (for example, see Fig. 1B). This shows that channel blocking by amiloride can be described in terms of simple, bimolecular kinetics, and that $k_1(R)$ in Eq. 4 is numerically negligible. The rate constant $k_2$ and the "apparent" constants $k_1' = k_1\beta$ and $K_A' = K_A/\beta$ can be estimated from the plot. We found $1/k_2$, the mean lifetime of the complex AR, to be in the order of 100 msec at room temperature. The apparent dissociation constant $K_A'$ was close to 1 $\mu M$ at 60 m$M$ $(Na)_o$. It decreased with decreasing $(Na)_o$, as expected if Na and amiloride compete for transport sites (*7*). The apparent constant $k_1'$ was found to be in the order of $10^7$ liter mole$^{-1}$ sec$^{-1}$ at 60 m$M$ $(Na)_o$.

For randomly blocked transport sites with unequal on and off probabilities (*5*) the plateau value of the power density spectrum (Eq. 2) is, in our notation, given by

$$S_0 = 4Mi^2P_oP_A\tau a \quad (5)$$

in which $a$ is the experimental membrane area. Substituting Eq. 1 into Eq. 5, we obtain

$$S_0 = 4I_{Na}P_A\tau ia \quad (5a)$$

Further combination with Eqs. 3a and 4a yields an expression for the amplitude of individual current pulses

$$i = \frac{S_0}{4aI_{Na}} \frac{k_1\beta}{(A)_o}[(A)_o + K_A']^2 \quad (6)$$

For $(Na)_o$ = 60 m$M$, values in the range 0.3 to 0.5 pa were computed, which correspond to turnover numbers of 1 to 3 × $10^6$ Na ions per second for individual transport sites. These turnover numbers are much larger than the values of $10^4$ ion/sec which are expected (*1*) and were observed (*8*) for shuttle-type mobile carriers, like valinomycin, which have to diffuse through the lipid phase of the membrane. Turnover rates of nonshuttle-type carriers, where the carrier molecule rotates or where only a part of the carrier molecule moves, have, to our knowledge, not yet been obtained experimentally. However, since such carriers will also have to overcome the viscosity and the electrostatic energy barrier of the lipid phase, low turnover rates will be expected in this case too. We feel justified, therefore, in concluding that in the Na-selective membrane of frog skin, transport occurs through pores, which are the only high-rate translocators presently known (*9*). This result is at variance with a previous conclusion by Biber and Sanders (*10*), who maintained that the Na transport is carrier mediated.

The mean density of open plus amiloride-blocked Na pores can be calculated from

$$M = I_{Na}/(iP_o) = 4aI_{Na}^2P_A\tau/(P_oS_o) \quad (7)$$

It was found to be in the range 0.7 to 2 × $10^8$ pores per square centimeter of membrane area at 60 m$M$ $(Na)_o$. When $(Na)_o$ was lowered to 15 m$M$ by substitution with K, larger pore densities were computed, but did not exceed 3 × $10^9$ pores per square centimeter. Extrapolation to $(Na)_o$ = 0 shows that the total number of pores ($N$) will be below 5 × $10^9$ cm$^{-2}$. This density corresponds to less than 50 pores per square micrometer of membrane area if a homogeneous distribution of pores over the apical membranes of all cells of the outer stratum granulosum may be assumed.

If, in the absence of amiloride, all pores were permanently open, a Na current $I_{Na} = iN = 2000$ $\mu$a/cm$^2$ would result at 60 m$M$ $(Na)_o$. This current is 75 times larger than the $I_{Na}$ value of 26 $\mu$a/cm$^2$ actually observed (see legend to Fig. 1A). We deduce from this observation that even in the absence of amiloride the pores are not permanently open (*11*).

B. LINDEMANN
*Second Department of Physiology, Universität des Saarlandes, 665 Homburg, West Germany*
W. VAN DRIESSCHE
*Laboratorium voor Fysiologie, 3000 Leuven, Belgium*

### References and Notes

1. C. M. Armstrong, *Biophys. J.* **15**, 932 (1975); *Q. Rev. Biophys.* **7**, 179 (1975).
2. We suggest that (i) the term carrier be applied only to translocators where the transfer-mediating moiety moves through the lipid phase; (ii) the term pore be applied to water-filled pathways that permit diffusional transport, which can, however, involve binding of ions to parts of the pore structure; and (iii) different terms be used for translocators that do not meet these specifications [see also (*9*)].
3. E. N. Ehrlich and J. Crabbé, *Pfluegers Arch.* **302**, 79 (1968).
4. Under short-circuit conditions, the voltage across the apical membrane will come even closer to the transepithelial voltage when the resistance of the apical membrane is increased by amiloride. Also, the decrease of $I_{Na}$ due to amiloride will decrease the K current of the K-selective, inward-facing membrane, and thus decrease the possible effect of this membrane on the recorded fluctuations. Finally, the intracellular Na concentration can be expected to become small in the presence of amiloride. This condition simplifies the computation of channel conductance.
5. A. A. Verveen and L. J. DeFelice, *Prog. Biophys. Mol. Biol.* **28**, 189 (1974).
6. G. H. Czerlinski, *Chemical Relaxation* (Dekker, New York, 1966); G. G. Hammes, *Adv. Protein Chem.* **23**, 1 (1968).
7. A. W. Cuthbert and W. K. Shum, *Naunyn Schmiedebergs Arch. Pharmakol.* **281**, 261 (1974); *Proc. R. Soc. London Ser. B* **189**, 543 (1975).
8. P. Läuger, "Carrier-mediated ion transport," *Science* **178**, 24 (1972).
9. Theoretically, translocators that combine properties of carriers and pores are conceivable. For instance, at a transport site the membrane may effectively be thinned down to a narrow protein structure, part of which can bind an ion selectively and transfer it by a rotational movement in low-viscosity surroundings ["translocase"; see P. Mitchell, *Nature (London)* **180**, 134 (1957)]. Transfer rates may be high, although this is not very likely in view of the low turnover numbers of most enzymes. H. Passow (personal communication) has estimated turnover numbers of $2 \times 10^4$ sec$^{-1}$ for the anion "carrier" of erythrocyte membranes, which might fulfill the structural requirements mentioned above. It is an open question of nomenclature how such translocators are to be classified. They resemble pores because the larger part of the membrane's diameter is passed by diffusion through a hydrophilic channel, and they resemble carriers because movement of a membrane component is essential for the transfer event. In the spirit of (*2*) we would not classify such structures, if they exist, as carriers. They may be viewed as pores in which the selectivity filter [B. Hille, *J. Gen. Physiol.* **58**, 599 (1971)] constitutes a peculiar energy barrier.
10. T. U. L. Biber and M. L. Sanders, *J. Gen. Physiol.* **61**, 529 (1973).
11. A. W. Cuthbert [*J. Physiol. (London)* **228**, 681 (1973)] computed, from amiloride binding data, a channel density of 400 $\mu$m$^{-2}$ [lower limit at 2.5 m$M$ $(Na)_o$], and from this calculated turnover rates for individual Na channels of 2000 sec$^{-1}$ at 2.5 m$M$ $(Na)_o$ and 8000 sec$^{-1}$ at 115 m$M$ $(Na)_o$ (upper limits). These turnovers are integrated over open and closed times of a channel and therefore cannot be directly compared with our results.
12. This work was supported by Deutsch Forschungegemeinschaft as project C1 within SFB 38, and by the Humboldt Foundation.

14 June 1976; revised 19 August 1976

## Size Limit of Molecules Permeating the Junctional Membrane Channels

Abstract. *The permeability of the cell-to-cell membrane channels in salivary gland cell junction* (Chironomus thummi) *was probed with fluorescent-labeled amino acids and synthetic or natural peptides. Molecules up to 1200 daltons pass through the channels with velocities depending on molecular size. Molecules of 1900 daltons or greater do not pass. This passage failure seems to reflect the normal size limit for junctional channel permeation; the channels continue to be permeated by the molecules up to 1200 daltons when these are mixed with the nonpermeant molecules. From this size limit a channel diameter of 10 to 14 angstroms is estimated.*

Since the finding that fluorescein, a molecule of 330 daltons, passes through a cell junction of low electrical resistance (*1*), other fluorescent and colorant substances have been used to probe junctional permeability properties (*2, 3*). However, the range of questions that could be studied has been restricted by the small number of useful probes available. We have now enlarged the repertoire of probes with the aim of determining the size limit of molecules permeating the junctional membrane channels (*4*).

We set out to construct fluorescent conjugates which incorporate some of the desirable features of the popular tracer fluorescein, such as water solubility, nontoxicity, low cytoplasmic binding, and high fluorescent yield. To obtain conjugates of well-defined structure, we sought, for the nonfluorescent backbone, not only a molecule of known structure but one with few reactive sites, preferably only one. Thus, the primary amine group of the synthetic and natural peptides listed in Table 1 was coupled with the fluorescent dyes fluorescein isothiocyanate (FITC), dansyl chloride (DANS), or lissamine rhodamine B (LRB) (*5*). The conjugation reactions were carried out at room temperature in an aqueous-acetone solvent made alkaline with $KHCO_3$. The products were purified by ion-exchange and gel-permeation chromatography. The criterion for purity was the formation of a single fluorescent spot in paper electrophoresis. Amino acid analysis and end-group analysis were performed on all peptides, except microperoxidase. The purified compounds were dissolved in water and the $p$H was adjusted to about 7 with KOH or HCl.

The solutions of the fluorescent probes were injected into cells of isolated *Chironomus* salivary glands (mid-fourth instar) with the aid of a micropipette and a pneumatic pressure system (*6*); the spread of the fluorescence inside the cells (excited with wavelengths of 460 nm for FITC, 340 nm for DANS, and 540 nm for LRB) was observed and photographed in a microscope darkfield, or, for velocity determinations, the spread was viewed and videotaped with the aid of an image intensifier-television system (*7*). The fluorescent emissions of FITC and DANS peak at 520 and 525 nm (yellow-green) and that of LRB, at 590 nm (red). Thus, in experiments where two tracers were injected together, the LRB was easily distinguished from either of the other two by the use of appropriate filters. In some cases, the tracer studies were combined with measurement of electrical coupling. Electrical current was then passed between the exterior and the interior of the cell injected with the tracer, and the resulting changes in membrane potential were measured in this cell and the immediate neighbor with the use of three microelectrodes (*1*).

The results obtained with the various tracers are summarized in Table 1. The amino acids and peptides with sizes less than or equal to 1158 daltons passed through the junction. Their fluorescence spread from the site of injection throughout the injected cell and into the cell neighbors at rates inversely related to molecular size. The tracers generally crossed several cell junctions on either side. The arrival of a tracer at the junction was marked by an abrupt change in the velocity of the fluorescence spread. With molecules less than or equal to 380 daltons, passage through the first junction became detectable within a few seconds of the tracer's arrival at the junction; and the fluorescence on the two sides of the junction appeared to equalize within 1 to 10 minutes. With molecules between 593 and 1158 daltons, the transit through junction was slower (tak-